Experimental Neurology 215 (2009) 243–252

Contents lists available at ScienceDirect

Experimental Neurology

journal homepage: www.elsevier.com/locate/yexnr

Posttraumatic epilepsy after controlled cortical impact injury in mice

Robert F. Hunt [a], Stephen W. Scheff [b,c,d], Bret N. Smith [a,*]

[a] Department of Physiology, University of Kentucky, MS-508 Chandler Medical Center, 800 Rose St., Lexington, KY 40536-0298, USA
[b] Department of Anatomy and Neurobiology, University of Kentucky, Lexington, KY 40536-0298, USA
[c] Sanders-Brown Center on Aging, University of Kentucky, Lexington, KY 40536-0298, USA
[d] Spinal Cord and Brain Injury Research Center, University of Kentucky, Lexington, KY 40536-0298, USA

ARTICLE INFO

Article history:
Received 27 May 2008
Revised 6 October 2008
Accepted 10 October 2008
Available online 26 October 2008

Keywords:
Traumatic brain injury
Seizures
Temporal lobe epilepsy
Hyperexcitability
Dentate gyrus
Mossy fiber sprouting

ABSTRACT

Many patients develop temporal lobe epilepsy after trauma, but basic mechanisms underlying the development of chronic seizures after head injury remain poorly understood. Using the controlled cortical impact injury model we examined whether mice developed spontaneous seizures after mild (0.5 mm injury depth) or severe (1.0 mm injury depth) brain injury and how subsequent posttraumatic mossy fiber sprouting was associated with excitability in the dentate gyrus 42–71 d after injury. After several weeks, spontaneous behavioral seizures were observed in 20% of mice with mild and 36% of mice with severe injury. Mossy fiber sprouting was typically present in septal slices of the dentate gyrus ipsilateral to the injury, but not in control mice. In slices with mossy fiber sprouting, perforant path stimulation revealed a significant reduction ($P<0.01$) in paired-pulse ratios in dentate granule cells at 20 ms and 40 ms interpulse intervals, but not at 80 ms or 160 ms intervals. These slices were also characterized by spontaneous and hilar-evoked epileptiform activity in the dentate gyrus in the presence of Mg^{2+}-free ACSF containing 100 μM picrotoxin. In contrast, paired-pulse and hilar-evoked responses in slices from injured animals that did not display mossy fiber sprouting were not different from controls. These data suggest the development of spontaneous posttraumatic seizures as well as structural and functional network changes associated with temporal lobe epilepsy in the mouse dentate gyrus by 71 d after CCI injury. Identifying experimental injury models that exhibit similar pathology to injury-induced epilepsy in humans should help to elucidate the mechanisms by which the injured brain becomes epileptic.

Introduction

Traumatic brain injury (TBI) is often accompanied by the delayed development of posttraumatic epilepsy (PTE) (Caveness et al., 1979; Annegers et al., 1998; Englander et al., 2003). PTE is manifested as temporal lobe epilepsy (TLE) in as many as 62% of trauma patients (Diaz-Arrastia et al., 2000; Hudak et al., 2004). However, prophylactic treatment for PTE has been largely unsuccessful and patients often do not qualify for surgery (Temkin et al., 1998, Temkin, 2001). Thus, a clinical association between TBI and epilepsy is well documented, but the cellular and molecular mechanisms by which trauma leads to the development of seizures remain poorly understood.

The dentate gyrus has long been regarded as a model system for studying alterations in synaptic circuitry associated with TLE (Tauck and Nadler, 1985; Sutula et al., 1989; Wuarin and Dudek, 1996; Buckmaster et al., 2002; Shibley and Smith, 2002). Experimental animal models and human TLE are characterized by hippocampal cell loss and mossy fiber sprouting in the dentate gyrus (Ben-Ari, 1985; Tauck and Nadler, 1985; Buckmaster et al., 2002; Shibley and Smith, 2002; Winokur et al., 2004; Jiao and Nadler, 2007). New recurrent excitatory circuits emerge after mossy fiber sprouting, and these changes are accompanied by increased excitability of the dentate gyrus and other limbic regions (Cronin and Dudek, 1988; Wuarin and Dudek, 1996, 2001; Smith and Dudek, 2001; Winokur et al., 2004). However, responses in TLE models may not reflect more subtle changes seen in human PTE. For example, status epilepticus induced by systemic administration of kainic acid or pilocarpine in rodents results in bilateral mossy fiber sprouting that is often much more robust than in hippocampi from surgical patients. Identifying experimental models of TBI that also display the pathophysiology of human TLE is necessary for understanding fundamental aspects of injury-induced epileptogenesis.

Several rodent models of TBI exist, but most are used to study acute or cognitive effects of brain injury and few have been adapted as animal models of TLE. Of these models, fluid percussion injury (FPI) and weight drop have been the most widely investigated as models of posttraumatic hyperexcitability. Studies performed in rats have suggested model-specific changes in seizure susceptibility, mossy fiber organization, and excitability after head injury that may also be

* Corresponding author. Fax: +1 859 323 1070.
E-mail address: bret.smith@uky.edu (B.N. Smith).

0014-4886/$ – see front matter © 2008 Elsevier Inc. All rights reserved.
doi:10.1016/j.expneurol.2008.10.005

related to injury severity and location (Golarai et al., 2001; Santhakumar et al., 2001; D'Ambrosio et al., 2004, 2005; Kharatishvili et al., 2006; Griesemer and Mautes, 2007). Controlled cortical impact (CCI) is a widely used experimental model of closed head injury that has not yet been identified as a model of injury-induced TLE. Several risk factors for epilepsy after trauma are modeled by lateral CCI including intraparenchymal hemorrhage accompanied by epidural and subdural hematomas (Lighthall, 1988; Dixon et al., 1991); cell loss in the neocortex, hippocampus, and dentate gyrus (Goodman et al., 1994; Smith et al., 1995; Fox et al., 1998; Anderson et al., 2005; Hall et al., 2005); neurogenesis in the dentate gyrus (Rola et al., 2006); and increases in morphologically identified synapses in the hippocampus (Scheff et al., 2005). Interestingly, early seizures within 24 h have sometimes been reported in this model (Nilsson et al., 1994; Kochanek et al., 2006). However, no data currently exists regarding chronic changes in excitability within the dentate gyrus after CCI.

In the present study we tested whether CCI can induce TLE and synaptic reorganization in the dentate gyrus in mice. Specifically, we focused on three main questions: (1) do mice develop spontaneous seizures; (2) does injury induce mossy fiber sprouting; and (3) are there long-term changes in excitability in the dentate gyrus after CCI injury?

Methods

Animals

Adult CD-1 mice (Harlan) weighing 25–30 g were housed under a normal 12 h light/12 h dark cycle. Water and food were available *ad libitum*. Mice were housed for a minimum of 7 d prior to experimentation. All procedures were approved by the University of Kentucky Animal Care and Use Committee.

Head trauma

Young-adult mice were subjected to a mild or severe unilateral cortical contusion by controlled cortical impact (CCI) as previously described (Scheff et al., 1997; Sullivan et al., 1999). Mice were anesthetized with isoflurane (2%) and placed in a stereotaxic frame. The skull was exposed by a midline incision, and a 4 mm craniotomy was made lateral to the sagittal suture and centered between bregma and lambda. The skull cap was removed without damage to the exposed underlying dura. The contusion device consisted of a computer controlled, pneumatically driven impactor fitted with a beveled stainless steel tip 3 mm in diameter (Precision Systems and Instrumentation, Fairfax, VA). Brain injury was delivered using this device to compress the cortex to a depth of 0.5 mm (mild) or 1.0 mm (severe) at a velocity of 3.5 m/s and 400 ms duration. Surgiseal (Johnson & Johnson, Arlington, TX) was placed over the dura after injury, the skull cap replaced, and the incision sutured.

Seizure assessment

Control and injured animals were monitored for seizures during 11 random 1–2 h intervals beginning 42 d post-injury until the day of experimentation (by 71 d). Five to eight mice were monitored per session for a total of 18 h. Each observation period included ~50% of mice from both mild and severe injury groups. Observation periods occurred during the light phase of the light/dark cycle, and seizures were rated from 1 to 5, with 5 being the most severe, according to a modified Racine scale as previously described (Racine, 1972; Shibley and Smith, 2002). To minimize subjectivity in seizure assessment, category one seizures (i.e. facial automatisms, increased grooming behaviors) were excluded since abnormalities of these behaviors are often difficult to distinguish.

Slice preparation

Mice were deeply anesthetized by isoflurane inhalation and decapitated. The brain was removed and stored for <1 min in ice-cold (2–4 °C) oxygenated artificial cerebrospinal fluid (ACSF) containing in mM: 124 NaCl, 3 KCl, 1.3 $CaCl_2$, 26 $NaHCO_3$, 1.3 $MgCl_2$, 1.25 NaH_2PO_4 and equilibrated with 95% O_2–5% CO_2 (pH 7.2–7.4). Brains were blocked, glued to a sectioning stage, and 400 μm-thick horizontal slices were cut in cold, oxygenated ACSF using a vibrating microtome (Vibratome Series 1000; Technical Products International, St. Louis, MO). The hippocampus was isolated from surrounding tissue, making sure to completely remove the entorhinal cortex. Slices were transferred to a storage chamber containing oxygenated ACSF at 34–36 °C and their order maintained so that the location along the septotemporal axis of each hippocampi was known. At least four slices from each animal were used for experiments: septal and temporal slices from both the ipsilateral and contralateral hemispheres.

Extracellular field potential recordings

Field potential recordings were obtained from the granule cell layer in the dentate gyrus 42–71 d post-CCI. For electrophysiological recording, slices were placed in recording chambers that allowed positioning of both stimulating and recording electrodes, and perfused with oxygenated ACSF. Slices were visualized under an upright microscope (Olympus BX51-WI) for electrode placement. Extracellular recording electrodes were filled with 1 M NaCl and placed near the apex of the granule cell layer for recordings. A concentric bipolar stimulating electrode made of platinum–iridium wire (125 μm diameter; FHC, Inc., Bowdoinham, ME) was used to apply stimuli to fiber pathways at 0.1 Hz. Stimulus intensity was adjusted to produce a population spike of ~50% of maximum amplitude. For antidromic stimulation experiments, a single stimulus was delivered to the hilus. For orthodromic activation experiments, pairs of stimuli were delivered to the perforant path at interpulse intervals (IPI) of 20, 40, 80, and 160 ms respectively and the ratio of the second population spike to the first (PS2/PS1) was calculated. An increase in the paired pulse ratio (PPR) of PS2/PS1 in slices from injury versus control groups was interpreted as a reduction in synaptic inhibition, and a reduction in the PPR was interpreted as an increase in synaptic inhibition (Reeves et al., 1997). Electrical signals were recorded using an Axopatch 200B amplifier (Axon Instruments), low-pass filtered at 2–5 kHz, digitized at 88 kHz (Neurocorder), stored on videotape, and analyzed on a PC computer using pClamp programs (Axon Instruments). In some experiments, slices were perfused with Mg^{2+}-free ACSF containing picrotoxin (100 μM) to block $GABA_A$-receptor mediated recurrent inhibition and unmask NMDA-receptor mediated excitatory synapses at resting membrane potential (Smith and Dudek 2001, 2002; Lynch and Sutula, 2000; Winokur et al., 2004).

Histology

Transverse hippocampal slices (i.e., horizontal with respect to brain orientation), including those used for recordings were placed in 0.37% sodium sulfide solution in 0.1 M $NaHPO_4$ for 20 min, followed by 4% paraformaldehyde in 0.15 M phosphate buffer for 1 h to fix the slices. Slices were then rinsed three times with phosphate buffered saline (PBS; 0.01 M; pH 7.4) and placed in a 30% sucrose solution in PBS overnight or until they sank for cryoprotection. The slices were sectioned at 20 μm on a cryostat, rinsed, mounted on charged slides (Superfrost Plus; Fisher Scientific), and dried overnight. Sections were treated according to previous protocols using Timm's stain to reveal mossy fibers and Nissl counterstained by cresyl violet to visualize cell bodies (Tauck and Nadler, 1985; Shibley and Smith, 2002). To quantify the regional distribution of mossy fiber sprouting after CCI, sections from the ipsilateral and contralateral hemispheres were examined by

an investigator who was blind to the electrophysiological outcomes at two locations along the septotemporal axis with respect to bregma: septal (~bregma −3.8 mm) and temporal (~bregma −6.5 mm). Scores for sprouting were assigned based on the following scale of Tauck and Nadler (1985): 0, little to no Timm granules in the granule cell layer; 1, mild staining in the granule cell layer but not the inner molecular layer; 2, moderate continuous staining through the granule cell layer with discontinuous, punctuate staining in the inner molecular layer; and 3, continuous band of dense staining throughout the inner molecular layer. At least three sections from each slice were examined and the median score reported if variability between sections existed. If Timm's staining between the blades of the granule cell layer was variable, an averaged score was used (e.g., if the lower blade had a score of 1 while the upper blade had a score of 2, the slice would be given an overall grade of 1.5). Timm scores >1 were considered to have an abnormal degree of mossy fiber sprouting (Patrylo and Dudek, 1998; Shibley and Smith, 2002).

Data analysis

Data were analyzed using Microsoft Excel and Instat. Numerical data are presented as the mean±S.E.M. Timm scores are represented as relative ranges. The nonparametric Kruskal–Wallis test with Dunn's *post hoc* was used to analyze for differences between groups of Timm scores. Electrophysiological data were analyzed by one-way ANOVA with Tukey's *post hoc*. Significance was set at $P<0.05$.

Results

Mice were subjected to either mild (0.5 mm injury depth; $n=10$) or severe (1.0 mm injury depth; $n=24$) CCI injury and compared to age-matched controls ($n=5$). Cortical contusion produced a consistent and reproducible focal lesion in the ipsilateral somatosensory cortex (Fig. 1A). This cortical site underwent substantial cell loss, as described in detail previously (Tong et al., 2002; Hall et al., 2005;

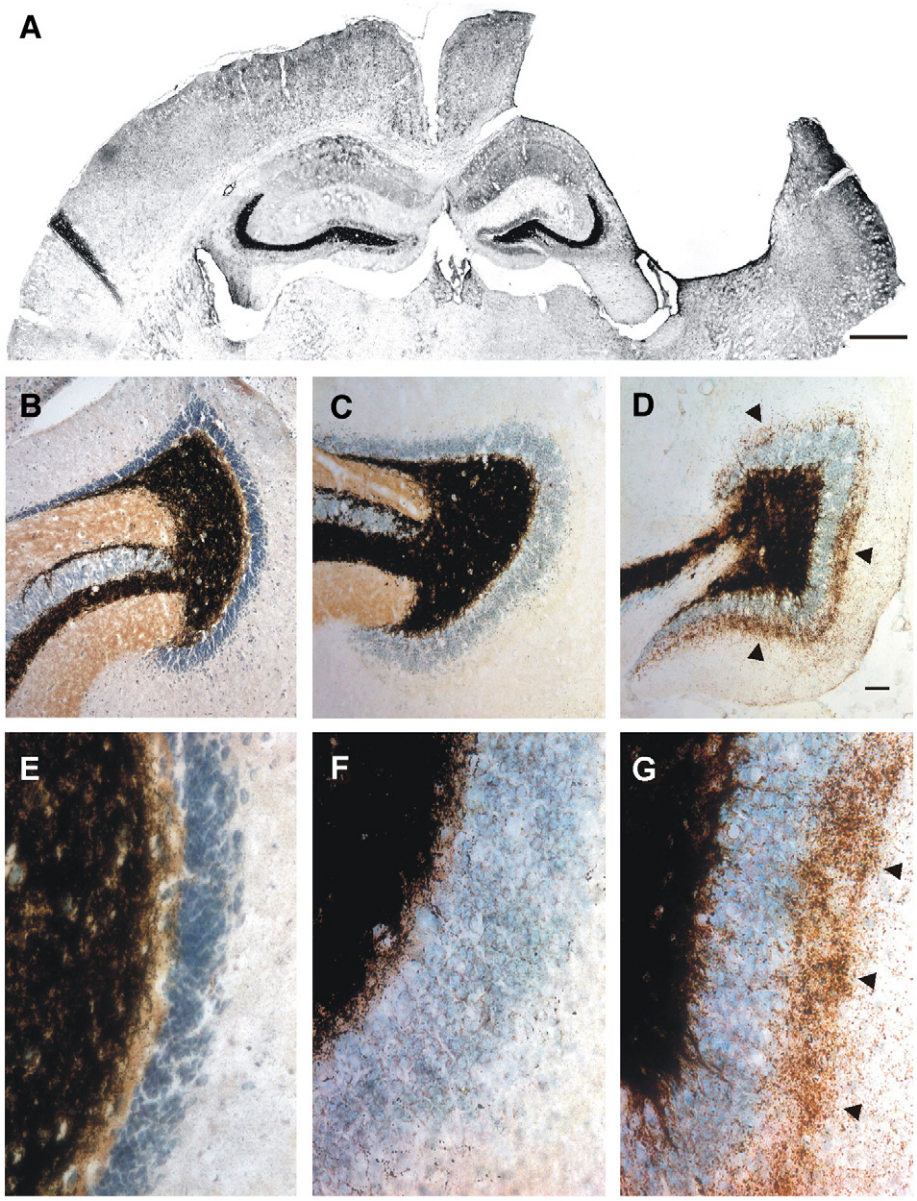

Fig. 1. Reorganization of mossy fiber projections after severe injury. (A) Representative Timm and Nissl counterstained coronal section (~Bregma −2.0 mm) from a mouse after severe controlled cortical impact TBI. (B) Timm and Nissl stained horizontal section from a control mouse. (C) Timm and nissl stained section from the contralateral hemisphere of an injured mouse 42 d post-CCI. (D) Staining in the septal dentate gyrus ipsilateral to the lesion revealed mossy fiber sprouting into the inner molecular layer (arrows) at the same septotemporal level and in the same mouse as in C. (E–G) Higher power images of B–D. Scale bars: 500 μm in A, 100 μm in B–D, 25 μm E–G.

Table 1
Development of seizures in CD-1 mice after controlled cortical impact

	Days post-injury	Survival rate (%)	Percent mice with seizures	Highest seizure category observed
Control	–	5/5 (100%)	0/5 (0%)	–
Mild injury (0.5 mm)	65.70±5.8[a]	10/10 (100%)	2/10 (20%)	2
Severe injury (1.0 mm)	61.18±8.55[a]	24/24 (100%)	4/11 (36%)	3

[a] Denotes mean±SD.

Saatman et al., 2006). All injured mice survived and remained otherwise healthy until the day of experimentation (Table 1).

Spontaneous seizures

Early posttraumatic seizures within 24 h after head-injury and acute increase of interstitial glutamate have previously been reported after CCI (Nilsson et al., 1994; Kochanek et al., 2006). However, delayed spontaneous seizures after CCI have not been described. Mice were passively monitored for spontaneous seizures beginning 42 d post-CCI until the day of experimentation (see Methods). Category 2 generalized seizures that included tail and neck stiffness, head nodding, and freezing up to 90 s or longer were observed in 20% (n=2 of 10) of mice that received mild injury and 36% (n=4 of 11) of mice that received severe injury (Table 1). Spontaneous tonic–clonic seizures that included single forelimb myoclonus (category 3) were also observed in two of 11 mice (18%) that sustained a severe injury.

Posttraumatic mossy fiber sprouting

Unprovoked generalized seizures after experimental brain trauma indicate limbic involvement (D'Ambrosio et al., 2005; Kharatishvili et al., 2006) and are associated with mossy fiber sprouting in murine models of TLE (Shibley and Smith, 2002). Timm's staining was performed on horizontal sections 7 d and 42–71 d after CCI to compare mossy fiber organization in septal and temporal hippocampal sections contralateral and ipsilateral to the lesion (see Methods). None of the 14 septal or temporal sections from 5 control animals contained abnormal mossy fiber organization (i.e. all Timm scores were <1; Figs. 1B, E). A Kruskal–Wallis test did not indicate a significant difference in Timm score distributions between groups at 7 d after severe injury in either septal ($H_{(2,\ 29)}$=5.262, P>0.05) or temporal ($H_{(2,\ 29)}$=0.954, P>0.05) dentate gyrus (Figs. 2A, B). However, two of 6 mice (33%) had aberrant mossy fiber sprouting (i.e. Timm scores>1) in septal sections of the dentate gyrus ipsilateral to the injury after 7 d. Mossy fiber sprouting was not observed in temporal sections or the contralateral hemisphere.

A Kruskal–Wallis test demonstrated a significant difference in Timm score ranges between groups 42–71 d after severe injury in both the septal ($H_{(2,\ 52)}$=23.453, P<0.0001) and temporal ($H_{(2,\ 52)}$=8.675, P<0.01) dentate gyrus (Figs. 2C, D). A Dunn's *post hoc* test demonstrated that Timm scores for ipsilateral slices were statistically different from controls at both septal and temporal locations (p<0.001). Of 18 mice, 10 (55%) contained mossy fiber sprouting in more septal sections (i.e. Timm score>1; Figs. 1D, G), and in two mice (11%) the sprouting was also observed in the temporal dentate gyrus.

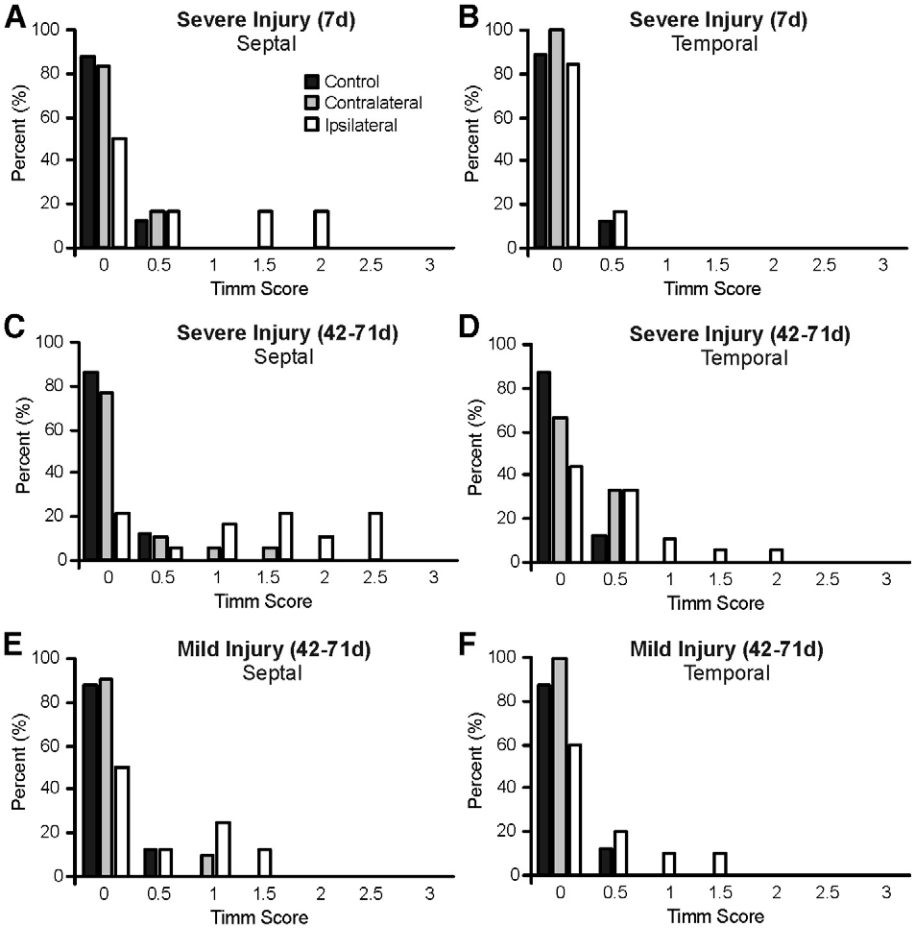

Fig. 2. Mossy fiber sprouting progresses with time after CCI injury. Sprouting was typically confined to the septal dentate gyrus of the ipsilateral hemisphere. Timm score ranges are given for three groups (controls, injured ipsilateral hemisphere, and injured contralateral hemisphere) from septal (A) and temporal (B) dentate gyrus 7 d after severe injury, septal (C) and temporal (D) dentate gyrus 42–71 d after severe injury, and septal (D) and temporal (E) dentate gyrus 42–71 d after mild injury.

Only one mouse (6%) had a Timm score>1 in the contralateral dentate gyrus 42–71 d post-injury (Figs. 1E, F). A small but significant difference in Timm score ranges was also found 42–71 d after mild injury in septal ($H_{(2,\ 36)}$=6.415, P<0.05) and temporal ($H_{(2,\ 37)}$=7.035, P<0.05) locations (Figs. 2D, E). However, a Dunn's *post hoc* test failed to find significant differences between groups. One mouse (10%) that received mild injury had moderate mossy fiber sprouting in the septal dentate gyrus, and one mouse (10%) contained moderate sprouting in the temporal dentate gyrus. None of these 10 mice were found to have abnormal mossy fiber organization in the contralateral hemisphere. The two mice that sustained severe injury and were observed to have spontaneous convulsive seizures also displayed robust mossy fiber sprouting (i.e. Timm scores>2.0) in the ipsilateral dentate gyrus after CCI. In all cases, the degree of sprouting decreased with temporal progression along the hippocampal axis.

In vitro electrophysiology

Responses to paired-pulse stimulation

Extracellular field recordings of perforant path input to dentate granule cells were used to assess the strength of synaptic inhibition in the dentate gyrus 42–71 d after CCI. Paired electrical stimuli were delivered to the perforant path at pairing intervals of 20, 40, 80, and 160 ms. The strength of inhibition was determined by measuring PPR – the amplitude of the second population spike as a percentage of the first (PS2/PS1) – of four experimental groups (septal and temporal slices of the dentate gyrus, ispilateral and contralateral to the lesion) after mild and severe injury compared to similarly located slices from controls. Responses in 14 hippocampal slices from 5 control animals revealed facilitation of the second population spike at all intervals (Fig. 3); a *t*-test confirmed no significant difference between septal-most and temporal slices from controls and the data were therefore combined for analysis. A one-way ANOVA demonstrated no significant change in PPR between the groups at any of the tested IPIs after either mild ($F_{(4,\ 59)}$=0.39, P>0.05, 20 ms; $F_{(4,57)}$=0.89, P>0.05, 40 ms; $F_{(4,65)}$=1.04, P>0.05, 80 ms; $F_{(4,56)}$=0.64, P>0.05, 160 ms) or severe ($F_{(4,\ 50)}$=0.66, P>0.05, 20 ms; $F_{(4,48)}$=1.00, P>0.05, 40 ms; $F_{(4,64)}$=1.71, P>0.05, 80 ms; $F_{(4,47)}$=2.36, P>0.05, 160 ms) CCI injury. No change in PPR was detected by selecting for injury only.

However, to determine whether granule cell responses were selectively altered in slices with mossy fiber sprouting, we further analyzed the PPR in slices of four different groups: (1) ipsilateral dentate gyrus with Timm scores≥1.5 (n=15 slices); (2) ipsilateral dentate gyrus with Timm scores≤1 (n=42 slices); (3) contralateral dentate gyrus (Timm scores≤1; n=46 slices); and (4) control dentate gyrus (Timm scores<1). A one-way ANOVA demonstrated a significant difference in PPR between groups at early IPIs of 20 ms and 40 ms ($F_{(3,\ 95)}$=4.13, P<0.01, 20 ms; $F_{(3,\ 93)}$=2.74, P<0.05, 40 ms) but not at 80 ms or 160 ms ($F_{(3,\ 118)}$=1.34, P>0.5, 80 ms; $F_{(3,\ 92)}$=0.67, P>0.05, 160 ms). *Post hoc* comparisons revealed that PPR was significantly reduced by 47% at the 20 ms interval and 59% at the 40 ms interval in ipsilateral slices that had mossy fiber sprouting (P<0.01), suggesting an increase in the strength of inhibition (Figs. 3A, B). Interestingly, PPR in slices from the ipsilateral hemisphere in injured animals that did not contain mossy fiber sprouting was not statistically different from controls at any IPI. Population spike amplitude ratios from the contralateral dentate gyrus, which also did not display mossy fiber sprouting, were also not different from controls (Figs. 3A, B).

Hyperexcitability in slices with mossy fiber sprouting

Hilar-evoked field potentials were examined in the same slices used to obtain paired-pulse data. These experiments were first performed in "normal" ACSF and then in Mg^{2+}-free ACSF containing 100 μM picrotoxin (PTX). In "normal" ACSF, electrical stimulation consistently elicited a single population spike in nearly all hippocampal slices from controls and injured animals (Figs. 4, 5A). Two ispilateral slices (one each from a mild and severe injury) had 2–3 population spikes. In Mg^{2+}-free ACSF containing PTX, a single population spike was elicited in all slices (n=14) from control animals (Fig. 4A). When hilar-evoked responses under these conditions were compared among injured animals, 98% (n=45 of 46) of contralateral slices without mossy fiber sprouting and 87.5% (n=35 of 40) of ipsilateral slices without mossy fiber sprouting had a single population spike (Fig. 4B). Three of 15 (20%) ipsilateral slices with mossy fiber sprouting had a single population spike similar to controls. Increased excitability or epileptiform activity was observed in the remaining slices, which almost exclusively included the ipsilateral dentate gyrus.

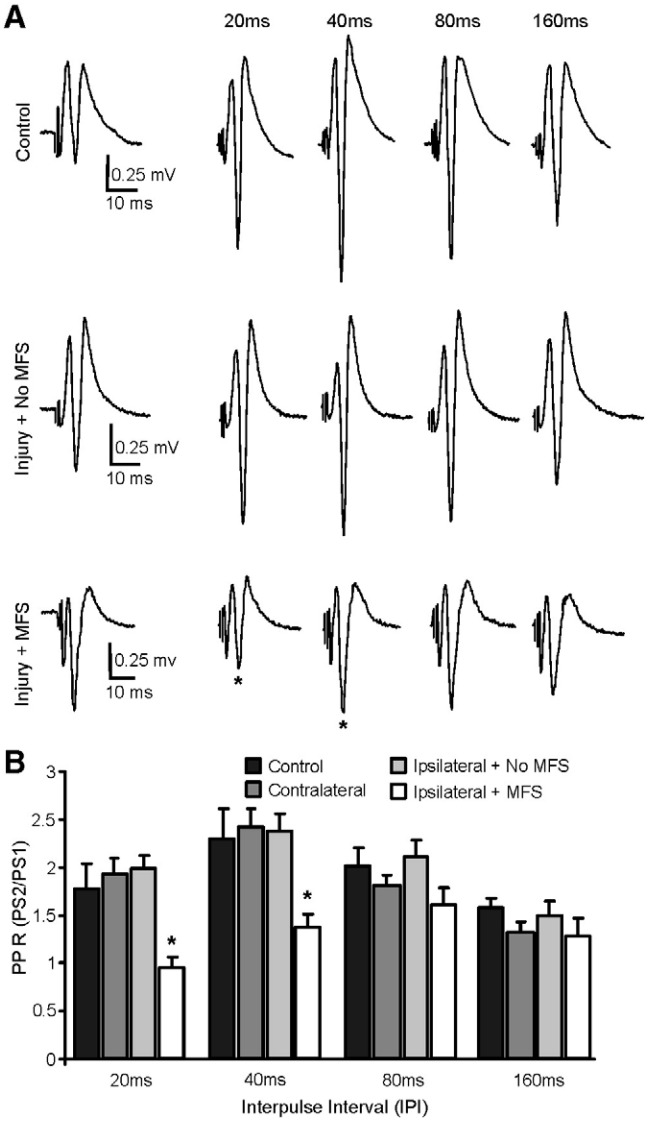

Fig. 3. Paired-pulse ratios in the dentate gyrus are reduced in slices from injured mice with mossy fiber sprouting 42–71 d after injury. (A) Representative field-potential recordings evoked by paired-pulsed stimulation of perforant path input to the dentate gyrus at 20, 40, 80, and 160 ms interpulse intervals in controls, CCI injured mice with no mossy fiber sprouting (MFS), and CCI injured mice with MFS. Facilitation of the second population spike was observed at all intervals in controls and injured mice without mossy fiber sprouting. Paired-pulse ratios were significantly decreased in slices from injured mice with mossy fiber sprouting at early (20 ms and 40 ms) but not later (80 ms and 160 ms) intervals. (B) Bar graph showing the mean PPR for all slices at 20, 40, 80, and 160 ms (n=15–46). Bars represent means±S.E.M. Asterisks (*) represent a significant reduction in paired-pulse ratios as determined by one-way ANOVA with Tukey's *post hoc* analysis (P<0.01).

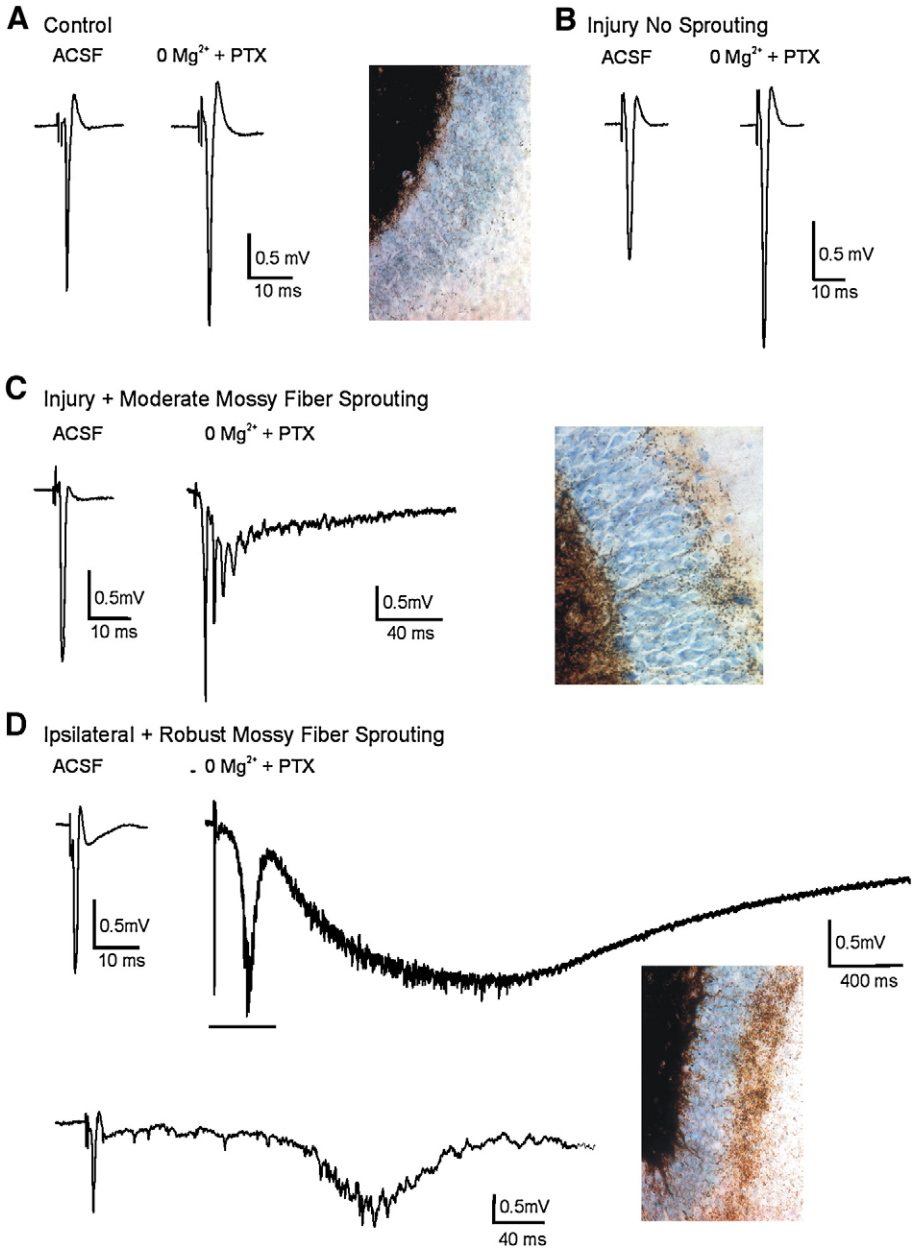

Fig. 4. Electrical stimulation of mossy fibers in the hilus evokes increased population responses in the dentate gyrus of mice with mossy fiber reorganization 42–71 d after CCI injury. (A, B) Hilar-evoked responses in controls and injured mice without mossy fiber sprouting consisted of a single population spike in normal ACSF and in Mg^{2+}-free ACSF containing PTX. (C) Evoked responses in a slice from a CCI-injured mouse with moderate mossy fiber sprouting. A single population spike was evoked in normal ACSF. Multiple population spikes were evoked in Mg^{2+}-free ACSF containing PTX. (D) Hilar stimulation evoked a single population spike in normal ACSF in a slice with robust mossy fiber sprouting. In Mg^{2+}-free ACSF containing PTX, a prolonged negative field-potential shift with secondary population activity was evoked. (D) The underlined portion of the trace in D is expanded below to demonstrate the initial population spike followed by secondary activity. Insets provide representative Timm's stains demonstrating the level of mossy fiber sprouting typical of slices that produced each response.

The increase in excitability was observed in the form of multiple population spikes in 1 (2%) contralateral slice, 5 (12.5%) ipsilateral slices without mossy fiber sprouting, and 12 (80%) ipsilateral slices with mossy fiber sprouting (Fig. 4C). In three (20%) of the slices from the ipsilateral dentate gyrus, hilar stimulation evoked prolonged negative-going field potentials and secondary population spikes with long and variable latency to the stimulus (Fig. 4D). Slices with the latter, most robust response, contained the highest degree of mossy fiber sprouting (Timm scores ≥ 2). Timm score ranges associated with a single population spike, multiple population spikes, and prolonged negative field shifts were compared and found to be statistically different by Kruskal–Wallis test ($H_{(2, 107)} = 27.77$, $P < 0.00001$; Fig. 5B). A Dunn's *post hoc* test confirmed that Timm scores associated with slices containing a single hilar-evoked population spike were significantly different from Timm scores of slices that had multiple population spikes ($P < 0.01$) and prolonged negative field shifts ($P < 0.001$). In both cases of hyperexcitability the secondary activity could be completely and reversibly blocked by 50 μM APV. The relative range of hilar-evoked responses observed in Mg^{2+}-free ACSF containing PTX for each experimental group are given in Fig. 5C.

Spontaneous epileptiform activity in slices with robust mossy fiber sprouting

The susceptibility to generation of spontaneous epileptiform activity in the presence of Mg^{2+}-free ACSF containing PTX was also

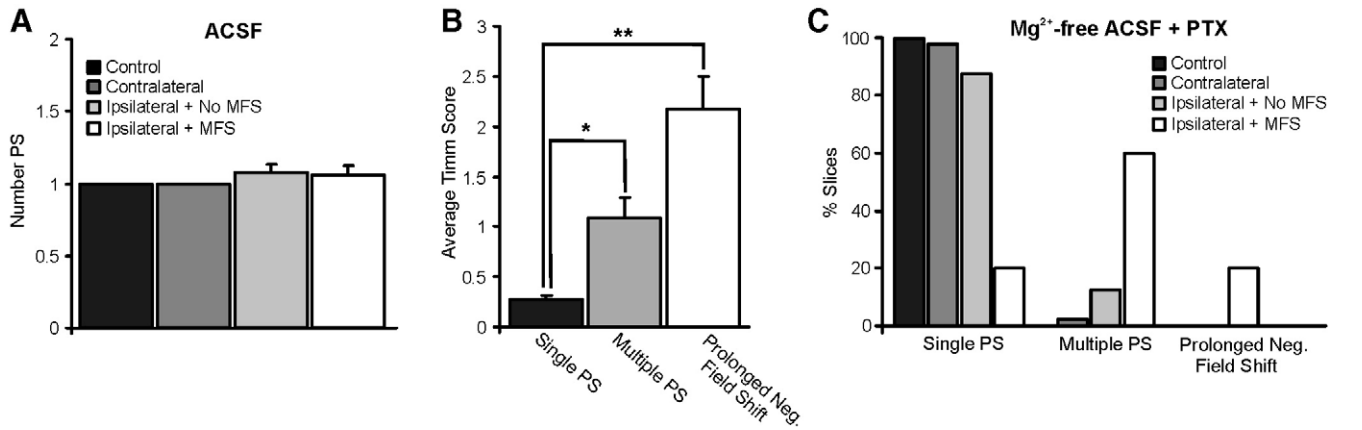

Fig. 5. Increased excitability is revealed in the dentate gyrus of CCI-injured mice during disinhibition. (A) Hilar stimulation in normal ACSF evoked a single population spike in nearly all slices from injured and control animals. (B) Average Timm scores for slices in which a single population spike, multiple population spikes, or prolonged negative field shifts were evoked in the presence of Mg^{2+}-free ACSF containing PTX. Bars represent means±S.E.M. Single asterisks (*) represent $P<0.01$ and double asterisks (**) represent a $P<0.001$ as determined by Kruskal–Wallis with Dunn's *post hoc* analysis. (C) Relative range of hilar-evoked population responses in Mg^{2+}-free ACSF containing PTX.

examined. Three ipsilateral slices that contained robust mossy fiber reorganization (i.e. Timm scores≥2) exhibited spontaneous bursts of population spikes and large amplitude negative-going field potential shifts of variable frequency in the granule cell layer (Fig. 6B). Small amplitude positive-going shifts, but not epileptiform burst discharges, were regularly observed in all other slices from injured and control animals (Fig. 6A).

Discussion

The results of this study suggest that the dentate gyrus of injured mice with mossy fiber sprouting became epileptogenic. Many mice developed spontaneous seizures by 42–71 d after mild or severe CCI injury, an important extension of previous studies that suggested this model of TBI induced early seizures (Nilsson et al., 1994; Kochanek et al., 2006). In addition, we found evidence for regionally localized structural reorganization of mossy fibers in the dentate gyrus ipsilateral to the injury that was accompanied by reduced PPR and increased spontaneous and hilar-evoked recurrent excitability. These long-term behavioral, anatomical, and functional changes are consistent with TLE development in humans and rodents.

Spontaneous seizures after mild and severe CCI

Several characteristics of seizures in our mice resembled seizures observed in other rodent models of TLE and PTE (Shibley and Smith, 2002; D'Ambrosio et al., 2004, 2005; Kharatishvili et al., 2006). In the present study, 20–36% of mice were observed to have unprovoked seizures weeks after injury. This is comparable to clinical studies that indicate as many as 39% of patients sustaining severe TBI with intact dura develop PTE (Caveness et al., 1979; Annegers et al., 1998). While increased seizure susceptibility to electrical stimulation and proconvulsant drug exposure has been noted after CCI and weight drop (Golarai et al., 2001; Statler et al., 2008), spontaneous seizures have only been reported in rats after severe FPI (Kharatishvili et al., 2006; Griesemer and Mautes, 2007). Previous studies have suggested that limbic involvement typically does not evolve in rats until several months after FPI (D'Ambrosio et al., 2004, 2005; Kharatishvili et al., 2006), but many mice in our study developed seizures and hippocampal pathology by 10 weeks post-injury. A shorter time period from injury to TLE makes studies of injury-induced epileptogenesis more feasible. Since animals in the present study were observed periodically, we presumably underestimated the number of

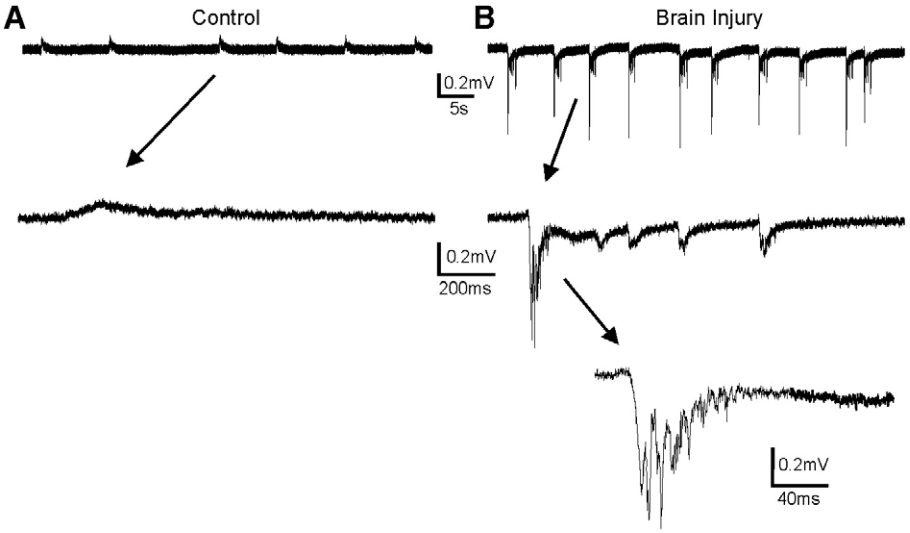

Fig. 6. Spontaneous population activity during disinhibition in slices from control and injured mice. (A) Field-potential recordings in the dentate gyrus of a control mouse demonstrate spontaneous positive-going field potential deflections. (B) Spontaneous epileptiform activity consisting of large amplitude negative going field shifts and spontaneous population spikes observed in the dentate gyrus of a mouse with mossy fiber sprouting. Arrows in A and B indicate expanded portions of the respective traces.

mice that developed spontaneous seizures and the frequency of seizures. However, we were mainly concerned with the qualitative assessment of seizure development after CCI. Continuous video-EEG or longer periods of seizure monitoring may increase the yield for seizure detection. It also remains to be elucidated whether a gradual shift in seizure type from partial to secondarily generalized over time also occurs after CCI as has been reported after FPI (D'Ambrosio et al., 2005; Kharatishvili et al., 2006).

Posttraumatic mossy fiber sprouting

Mossy fiber reorganization is a phenomenon repeatedly observed in TLE patients and animal models, is well developed by 2–4 weeks after an epileptogenic insult in rodents, and persists throughout life (Dudek and Spitz, 1997). Mossy fiber sprouting may only be one of many anatomical factors such as neuron loss, neurogenesis, gliosis, or morphological changes associated with epileptogenesis (Pitkanen and Sutula, 2002). However, we examined changes in mossy fiber organization because of its traditional consistency and reliability as a marker of the epileptic dentate gyrus. Mossy fiber sprouting after CCI was most prominent in dorsal regions of the ipsilateral dentate gyrus and resembled sprouting observed in humans and animal models of TLE (Tauck and Nadler, 1985; Shibley and Smith, 2002). Previous reports in rats have indicated minimal sprouting in the dentate gyrus ipsilateral to the injury at 3 months post-FPI (Santhakumar et al., 2001) and dense sprouting in the septal dentate gyrus ipsilateral to the injury in rats that display spontaneous seizures by 12 months (Kharatishvili et al., 2006). However, we detected minimal axon reorganization near the injury site as early as 7 d post-injury, and the number of animals with mossy fiber sprouting increased with time post-injury such that 55% of mice were found to have locally abnormal mossy fiber organization by 10 weeks after severe CCI. Even in animals with spontaneous seizures, mossy fiber sprouting was mainly localized to areas ipsilateral and proximal to the lesion. Thus, sprouting may not need to be as widespread as is often observed in status epilepticus-induced TLE models to contribute to seizures.

Injury severity may contribute to the degree of mossy fiber sprouting after TBI. Similar to the observation that severe lateral FPI is necessary to induce sprouting in rats (Santhakumar et al., 2001), more mice developed mossy fiber sprouting after severe CCI. Several previous studies have described in detail the extent, variability, and progression of cortical and hippocampal damage after mild or severe CCI in mice (Hannay et al., 1999; Tong et al., 2002; Hall et al., 2005; Saatman et al., 2006). Previous reports in rats and mice indicate greater cortical lesion volume after severe versus mild injury that is due to an increase in injury depth but not rostral–caudal extent of the injury (Goodman et al., 1994; Hannay et al., 1999; Saatman et al., 2006). The present electrophysiological experiments utilized mainly horizontal slices, which allowed recordings to be made from approximately the temporal two-thirds of the hippocampal formation (i.e., from just ventral to the lesion to near the temporal pole), so the lesion site itself was not analyzed. Since our methods of CCI were identical to those used in previous studies (Hall et al., 2005), the assumption is that the initial lesion was similar in dimension and variability to that described previously. Despite reports that indicate severe injury in the CCI model can occasionally produce bilateral damage to structures that are especially susceptible to injury, such as the thalamus and hippocampus (Goodman et al., 1994; Smith et al., 1995), nearly all slices from the contralateral dentate gyrus appeared devoid of mossy fiber sprouting in the inner molecular layer, even in mice with generalized seizures. Thus, it is possible to observe a full range of Timm scores – from no sprouting to robust sprouting – in slices from a single mouse after CCI.

The presence of regionally robust mossy fiber sprouting in mice that displayed category 3 seizures suggests an association between axon sprouting and seizure severity and/or frequency after TBI. However, it is difficult to establish whether injury-induced mossy fiber reorganization precipitates limbic seizures, seizures induce mossy fiber sprouting, a combination of the two occur, or even to be confident that sprouting is a necessary accompaniment of limbic seizures. Studies aimed at determining causality are complicated by the myriad cellular and molecular alterations occurring concurrent with axon sprouting, several of which may also contribute to the development of seizures after brain injury. Synaptic reorganization in other damaged structures such as CA1, amygdala, and neocortex could additionally contribute to seizure development after injury but are more difficult to detect. For example, increases in synaptic connections and excitability of CA1 pyramidal cells have been reported after focal injury (i.e. CCI and weight drop), are also seen in TLE models, and could further contribute to seizures (Smith and Dudek, 2001; 2002; Scheff et al., 2005; Griesemer and Mautes, 2007). Moreover, Buckmaster and Dudek (1997b) reported no direct association between seizure frequency and the degree of mossy fiber sprouting after kainate-treatment. In the present study sprouting was more prevalent at 42–71 d versus 7 d after severe CCI injury, suggesting progressive development of new excitatory connections in the dentate gyrus. However, mice were not monitored for seizures at the earlier time points, and the relationship between structural damage, axon sprouting, and seizure development was beyond the scope of this study. Further investigations using continuous EEG in combination with cellular techniques that compare animal models with variable levels of mossy fiber sprouting (i.e., TBI, status epilepticus, etc.) may provide insight into any causal relationships between axon sprouting, epileptogenesis, and the onset of limbic seizures.

Increased synaptic inhibition after CCI

Reduced PPR has been repeatedly demonstrated in the dentate gyrus of epileptic patients and animal models of TLE (Tuff et al., 1983; Buckmaster and Dudek, 1997a; Swanson et al., 1998). One view is that mossy fiber sprouting after an epileptogenic insult plays a restorative role by enhancing excitatory synaptic input onto GABAergic interneurons in the hilus (Sloviter, 1991, 1992). However, other studies have demonstrated decreased inhibitory input onto granule cells that is possibly related to the loss of GABAergic interneurons in epileptic animals (Buckmaster and Dudek, 1997a; Kobayashi and Buckmaster, 2003). Previous reports of paired-pulse data in rats after TBI have been conflicting. Reeves et al. (1997) reported reduced PPR in the ipsilateral dentate gyrus at early IPIs (20 ms–100 ms) up to 15 d post-FPI *in vivo*. Other studies have suggested no change or even increased PPR weeks to months after TBI (Lowenstein et al., 1992; Golarai et al., 2001). In the present study, PPR at all IPIs from ipsilateral and contralateral slices without mossy fiber sprouting was similar to controls. We found that PPR was selectively reduced at earlier (20 ms and 40 ms) but not later (80 ms and 160 ms) IPIs in slices with mossy fiber sprouting (Timm scores>1) after injury. This is an interesting finding that suggests a long-term increase in synaptic inhibition after TBI associated with mossy fiber reorganization. Previous studies of posttraumatic hyperexcitability have not differentiated between slices with and without sprouting. Perforant path stimulation did not consistently evoke paired pulse inhibition at low IPIs (i.e., 20 ms) in control slices as is commonly observed. However, other reports demonstrated paired-pulse facilitation in control slices at low IPIs (Kirby et al., 1995; Hirota and Roth, 1997). Differences in stimulation frequency, intensity, interpulse interval, time post-injury, ACSF composition, and/or animal model could all contribute to discrepancies among studies. Moreover, variations in stimulus parameters have been reported to have inconsistent effects on paired-pulse inhibition, particularly at high stimulation frequencies and/or intensities (Waldbaum and Dudek, 2005, 2007). In the present study all experimental conditions remained constant; control data were obtained alongside data from injured animals, and different slices from injured animals were

treated identically within an experiment. Field-potential experiments are limited in that perforant path stimulation is not a direct measure of GABA-mediated inhibition. We found that interval-specific changes in PPR was associated with mossy fiber sprouting, consistent with the hypothesis that sprouting may increase synaptic inhibition in these slices, but it remains possible that other injury-induced changes of dentate gyrus networks could produce similar effects. Alternative interpretations of our paired-pulse data could include the possibility of a presynaptic effect such that transmitter release probability is altered, inhibitory cells may sustain damage and undergo functional changes as a result of TBI, and/or hilar mossy cells may be driving synaptic inhibition in the injured mice. Future experiments that use cellular approaches to assess excitatory and inhibitory drive onto both granule cells and GABAergic interneurons may better clarify the effect of TBI on recurrent inhibition in the dentate gyrus. Regardless, our data suggest an interval-specific and selective reduction of PPR in slices containing mossy fiber sprouting after TBI.

Epileptiform activity after CCI

Numerous *in vitro* studies have suggested that mossy fiber reorganization contributes to epileptiform activity and seizures by forming a positive-feedback network among granule cells (Cronin and Dudek, 1988; Molnar and Nadler, 1999; Lynch and Sutula, 2000; Buckmaster et al., 2002; Scharfman et al., 2003; Winokur et al., 2004). Our data are consistent with this view. An increased susceptibility to spontaneous and evoked epileptiform activity in the ipsilateral dentate gyrus of slices with mossy fiber sprouting were revealed in the presence of Mg^{2+}-free ACSF containing PTX. These epileptiform discharges were not observed in slices from injured or control animals that did not display mossy fiber sprouting. Spontaneous positive shifts in slices from controls and negative field shifts in slices from kainate treated rats and reeler mutant mice during disinhibition have previously been described (Wuarin and Dudek, 1996; Buckmaster and Dudek, 1997a; Patrylo et al., 2006). Hilar stimulation evoked prolonged negative-going field-potential shifts and secondary population spikes in slices with robust levels of sprouting and multiple population spikes in many but not all slices with more moderate levels of mossy fiber sprouting. These responses are qualitatively similar to those observed in animal models of TLE (Tauck and Nadler, 1985; Cronin et al., 1992; Wuarin and Dudek, 1996; Patrylo and Dudek, 1998; Winokur et al., 2004). Multiple population spikes were observed in a small percentage of ipsilateral and contralateral slices that did not have robust mossy fiber sprouting. This may indicate that mossy fiber reorganization is not solely responsible for the enhanced excitability in some slices. However, one obvious limitation to electrical stimulation is that cell bodies and other axons of passage can be activated concurrent with mossy fibers making it an indirect measurement of synaptic connectivity. The possibility that neurons in the hilus (e.g., excitatory mossy cells) play a role in the increased excitability observed in our preparation cannot be excluded. Caged glutamate microstimulation (Molnar and Nadler, 1999; Wuarin and Dudek, 2001; Winokur et al., 2004) or dual intracellular recordings (Scharfman et al., 2003) could provide a more direct assessment of synaptic connections between granule cells after CCI. Even so, our data indicate that mossy fiber reorganization in slices from injured animals is associated with increased susceptibility for epileptiform activity.

Additional comparisons between CCI and other experimental models of TBI-induced epilepsy

Distinct strengths and limitations exist with any experimental model. Currently, FPI and weight drop are the most widely used trauma models that have also been adapted as models of posttraumatic hyperexcitability. CCI offers potential advantages over these other models. Perhaps the most important advantage is that CCI has been adapted to mice (Smith et al., 1995; Sullivan et al., 1999), rats (Dixon et al., 1991; Scheff et al., 1997), and even larger animals such as sheep (Anderson et al., 2003). To date, studies of TBI-induced epilepsy using FPI and weight drop have been nearly exclusively performed in rats. The ability to perform CCI in mice provides an invaluable experimental tool for studying the contribution of genetic background in PTE development. CCI produces a consistent and reproducible focal injury in each animal, and mechanical parameters (i.e., injury velocity, depth, and tissue deformation) are easily managed. There is minimized risk for inaccuracy or secondary "rebound" injury as can be seen with other focal TBI models (i.e., weight drop). On the other hand, lateral FPI produces a mixed focal *and* diffuse injury making it impossible to determine the contribution of each injury type to epileptogenesis. A more focused and consistent injury produced in CCI may have behavioral and/or functional implications. One commonality among the abovementioned TBI models is that all produce a degree of focal injury. This suggests that focal injury may play a more critical role in epileptogenesis than diffuse injury. Thus, the highly focal lesion produced by CCI may reflect a more relevant aspect of PTE. A potential limitation of the CCI model is that increasing injury severity does not achieve increased mortality; this contradicts clinical observations. Severity of lateral FPI must be increased such that mortality rate is ~50% in order to induce TLE in rats (Kharatishvili et al., 2006). Mortality after severe FPI may be due to disproportionate injury to the brainstem and/or the more diffuse nature of the model. Weight drop is another highly focal model of severe TBI after which nearly all animals have been similarly reported to survive (Griesemer and Mautes, 2007). Therefore, the injury-induced sequence of events leading to mortality may be different from those leading to TLE.

In conclusion, CCI reproduced key behavioral, anatomical, and functional features common to human PTE and TLE in mice. Development of specific hippocampal pathology often associated with TLE development occurred at earlier time points than described in some other TBI models. Therefore, CCI not only provides a useful model of TBI but is also effective in inducing PTE in mice.

Acknowledgments

This research was supported by NIH NS052302 to B.N.S., NIH AG21981 to S.W.S., and an Epilepsy Foundation Training Fellowship to R.F.H. We wish to thank Kelly Roberts for technical assistance with the injury models.

References

Anderson, K.J., Miller, K.M., Fugaccia, I., Scheff, S.W., 2005. Regional distribution of Fluoro-Jade B staining in the hippocampus following traumatic brain injury. Exp. Neurol. 193, 125–130.
Anderson, R.W., Brown, C.J., Blumbers, P.C., McLean, A.J., Jones, N.R., 2003. Impact mechanics and axonal injury in a sheep model. J. Neurotrauma 20, 961–974.
Annegers, J.F., Hauser, A., Coan, S.P., Rocca, W.P., 1998. A population-based study of seizures and traumatic brain injuries. N. Eng. J. Med. 338, 20–24.
Ben-Ari, Y., 1985. Limbic seizure and brain damage produced by kainic acid: mechanisms and relevance to human temporal lobe epilepsy. Neurosci. 14, 375–403.
Buckmaster, P.S., Zhang, G.F., Yamawaki, R., 2002. Axon sprouting in a model of temporal lobe epilepsy creates a predominantly excitatory feedback circuit. J. Neurosci. 22, 6650–6658.
Buckmaster, P.S., Dudek, F.E., 1997a. Network properties of the dentate gyrus in epileptic rats with hilar neuron loss and granule cell axon reorganization. J. Neurophysiol. 77, 2596–2685.
Buckmaster, P.S., Dudek, F.E., 1997b. Neuron loss, granule cell axon reorganization, and functional changes in the dentate gyrus of epileptic kaintate treated rats. J. Comp. Neurol. 385 385:404.
Caveness, W.F., Meirowski, A.M., Rish, B.L., Mohr, J.P., Kistler, J.P., Dillon, J.D., Weiss, G.H., 1979. The nature of posttraumatic epilepsy. J. Neurosurg. 50, 545–553.
Cronin, J., Dudek, F.E., 1988. Chronic seizures and collateral sprouting of dentate mossy fibers after kainic acid treatment in rats. Brain Res. 474, 181–184.
Cronin, J., Obenaus, A., Houser, C.R., Dudek, F.E., 1992. Electrophysiology of dentate granule cells after kainite-induced synaptic reorganization of the mossy fibers. Brain Res. 573, 305–310.
D'Ambrosio, R., Fairbanks, J.P., Fender, J.S., Born, D.E., Doyle, D.L., Miller, J.W., 2004. Post-traumatic epilepsy following fluid percussion injury in the rat. Brain 127, 304–314.

D'Ambrosio, R., Fender, J.S., Fairbanks, J.P., 2005. Progression from frontal–parietal to mesial–temporal epilepsy after fluid percussion injury in the rat. Brain 128, 174–188.
Diaz-Arrastia, R., Agostini, M.A., Frol, A.B., Mickey, B., Fleckenstein, J., Bigio, E., Van Ness, P.C., 2000. Neurophysiologic and neuroradiologic features of intractable epilepsy after traumatic brain injury in adults. Arch. Neurol. 57, 1611–1616.
Dixon, C.E., Clifton, G.L., Lighthall, J.W., Yaghmai, A.A., Hayes, L., 1991. A controlled cortical impact model of traumatic brain injury in the rat. J. Neurosci. Methods 3, 253–262.
Dudek, F.E., Spitz, M., 1997. Hypothetical mechanisms for the cellular and neurophysiologic basis of secondary epileptogenesis: proposed role of synaptic reorganization. J. Clin. Neurophysiol. 14, 90–101.
Englander, J.E., Bushnik, T., Duong, T.T., Cifu, D.X., Zafonte, R., Wright, J., Hughes, R., Bergman, W., 2003. Analyzing the risk factors for late posttraumatic seizures: a prospective, multicenter investigation. Arch. Phys. Med. Rehabil. 84, 365–373.
Fox, G.B., Fan, L., Levasseur, R.A., Faden, A.I., 1998. Sustained sensory/motor and cognitive deficits with neuronal apoptosis following controlled cortical impact brain injury in the mouse. J. Neurotrauma 15, 599–614.
Golarai, G., Greenwood, A.C., Feeney, D.M., Connor, J.A., 2001. Physiological and structural evidence for hippocampal involvement in persistent seizure susceptibility after traumatic brain injury. J. Neurosci. 21 (21), 8523–8537.
Goodman, J.C., Cherian, L., Bryan Jr, R.M., Robertson, C.S., 1994. Lateral cortical impact injury in rats. Pathologic effects of varying cortical compression and impact velocity. J. Neurotrauma 11, 587–597.
Griesemer, D., Mautes, A.M., 2007. Closed head injury causes hyperexcitability in rat hippocampal CA1 but not in CA3 pyramidal cells. J. Neurotrauma 24, 1823–1832.
Hall, E.D., Sullivan, P.G., Gibson, T.R., Pavel, K.M., Thompson, B.M., Scheff, S.W., 2005. Spatial and temporal characteristics of neurodegeneration after controlled cortical impact in mice: more than a focal brain injury. J. Neurotrauma 22 (2), 252–265.
Hannay, H.J., Feldman, Z., Phan, P., Keyani, A., Panwar, N., Goodman, J.C., Robertson, C.S., 1999. Validation of a controlled cortical impact model of head injury in mice. J. Neurotrauma 16, 1103–1114.
Hirota, K., Roth, S.H., 1997. The effects of sevoflurane on population spikes in CA1 and dentate gyrus of the rat hippocampus in vitro. Anesth. Analg. 85, 426–430.
Hudak, A.M., Trivedi, K., Harper, C.R., Booker, K., Caesar, R.R., Agostini, M., Van Ness, P.C., Diaz-Arrastia, R., 2004. Evaluation of seizure-like episodes in survivors of moderate and severe traumatic brain injury. J. Head Trauma Rehabil. 19, 290–295.
Jiao, Y., Nadler, J.V., 2007. Stereological analysis of GluR2-immunoreactive hilar neurons in the pilocarpine model of temporal lobe epilepsy: correlation of cell loss with mossy fiber sprouting. Exp. Neurol. 205, 569–582.
Kharatishvili, I., Nissinen, J.P., McIntosh, T.K., Pitkänen, A., 2006. A model of posttraumatic epilepsy induced by lateral fluid-percussion brain injury in rats. Neuroscience 140, 685–697.
Kirby, M.T., Hampson, R.E., Deadwyler, S.A., 1995. Cannabinoids selectively decrease paired-pulse facilitation of perforant path synaptic potentials in the dentate gyrus in vitro. Brain Res. 688, 114–120.
Kobayashi, M., Buckmaster, P.S., 2003. Reduced inhibition of dentate granule cells in a model of temporal lobe epilepsy. J. Neurosci. 23, 2440–2452.
Kochanek, P.M., Vagni, V.A., Janesko, K.L., Washington, C.B., Crumrine, P.K., Garman, R.H., Jenkins, L.W., Clark, R.S., Homanics, G.E., Dixon, C.E., Schnermann, J., Jackson, E.K., 2006. Adenosine A1 receptor knock-out mice develop lethal status epilepticus after experimental traumatic brain injury. J. Cerebral. Blood Flow Met. 26, 565–575.
Lighthall, J.W., 1988. Controlled cortical impact: a new experimental brain injury model. J Neurotrauma 5, 1–15.
Lowenstein, D.H., Thomas, M.J., Smith, D.H., McIntosh, T.K., 1992. Selective vulnerability of dentate hilar neurons following traumatic brain injury: a potential mechanistic link between head trauma and disorders of the hippocampus. J. Neurosci. 12, 4846–4853.
Lynch, M., Sutula, T., 2000. Recurrent excitatory connectivity in the dentate gyrus of kindled and kainic acid-treated rats. J. Neurophysiol. 83, 604–693.
Molnar, P., Nadler, J.V., 1999. Mossy fiber-granule cell synapses in the normal and epileptic rat dentate gyrus studied with minimal laser photostimulation. J. Neurophysiol. 82, 1883–1894.
Nilsson, P., Ronne-Engstrom, E., Flink, R., Ungersted, U., Carlson, H., Hillered, L., 1994. Epileptic seizure activity in the acute phase following cortical impact trauma in rat. Brain Res. 637, 227–232.
Patrylo, P.R., Dudek, F.E., 1998. Physiological unmasking of new glutamatergic pathways in the dentate gyrus of hippocampal slices from kainate-induced epileptic rats. J. Neurophysiol. 79, 418–429.
Patrylo, P.R., Browning, R.A., Cranick, S., 2006. Reeler homozygous mice exhibit enhanced susceptibility to epileptiform activity. Epilepsia 47, 257–266.
Pitkanen, A., Sutula, T.P., 2002. Is epilepsy a progressive disorder? Prospects for new therapeutic approaches in temporal lobe epilepsy. Lancet Neurol. 1, 173–181.
Racine, R.J., 1972. Modification of seizure activity by electrical stimulation: II. Motor seizures. Electrorencephalogr. Clin. Neurophysiol. 32, 281–294.
Reeves, T.M., Lyeth, B.G., Phillips, L.L., Hamm, R.J., Povlishock, J.T., 1997. The effects of traumatic brain injury on inhibition in the hippocampus and dentate gyrus. Brain Res. 1, 119–132.
Rola, R., Mizumatsu, S., Otsuka, S., Morhardt, D.R., Noble-Haeusslein, L.J., Fishman, K., Potts, M.B., Fike, J.R., 2006. Alterations in hippocampal neurogenesis following traumatic brain injury in mice. Exp. Neurol. 202, 189–199.
Saatman, K.E., Feeco, K.J., Pape, R.L., Raghupathi, R., 2006. Differential behavioral and histopathological responses to graded cortical impact injury in mice. J. Neurotrauma 23, 1241–1253.
Santhakumar, V., Ratzliff, A.D.H., Jeng, J., Toh, Z., Soltesz, I., 2001. Long-term hyperexcitability in the hippocampus after experimental head trauma. Ann. Neurol. 50, 708–717.
Scharfman, H.E., Sollas, A.L., Berger, R.E., Goodman, J.H., 2003. Electrophysiological evidence of monosynaptic excitatory transmission between granule cells after seizure-induced mossy fiber sprouting. J. Neurophysiol. 90, 2536–2547.
Scheff, S.W., Baldwin, S.A., Brown, R.W., Kraemer, P.J., 1997. Morris water maze deficits in rats following traumatic brain injury: lateral controlled cortical impact. J. Neurotrauma 14, 615–627.
Scheff, S.W., Price, D.A., Hicks, R.R., Baldwin, S.A., Robinson, S., Brackney, C., 2005. Synaptogenesis in the hippocampal CA1 field following traumatic brain injury. J. Neurotrauma 22, 719–732.
Shibley, H., Smith, B.N., 2002. Pilocarpine-induced status epilepticus results in mossy fiber sprouting and spontaneous seizures in C57BL/6 and CD-1 mice. Epilepsy Res. 49, 109–120.
Sloviter, R.S., 1991. Permanently altered hippocampal structure, excitability, and inhibition after experimental status epilepticus in the rat: the "dormant basket cell" hypothesis and its possible relevance to temporal lobe epilepsy. Hippocampus 1 (1), 41–66.
Sloviter, R.S., 1992. Possible functional consequences of synaptic reorganization in the dentate gyrus of kainite-treated rats. Neurosci. Lett 137, 91–96.
Smith, B.N., Dudek, F.E., 2001. Short- and long-term changes in CA1 network excitability after kainate treatment in rats. J. Neurophysiol. 85, 1–9.
Smith, B.N., Dudek, F.E., 2002. Network interactions mediated by new excitatory connections between CA1 pyramidal cells in rats with kainite-induced epilepsy. J. Neurophysiol. 87, 1655–1658.
Smith, D.H., Soares, H.D., Pierce, J.E.S., Perlman, K.G., Saatman, K.E., Meaney, D.F., Dixon, C.E., McIntosh, T.K., 1995. A model of parasagittal controlled cortical impact in the mouse cognitive and histopathologic effects. J. Neurotrauma 12, 169–178.
Statler, K.D., Swank, S., Abildskov, T., Bigler, E.D., White, H.S., 2008. Traumatic brain injury during development reduces minimal clonic seizure thresholds at maturity. Epilepsy Res. 80, 163–170.
Sullivan, P.G., Bruce-Keller, A.J., Rabchevsky, A.G., Christakos, S., St. Clair, D.K., Mattson, M.P., Scheff, S.W., 1999. Exacerbation of damage and altered NFkB activation in mice lacking tumor necrosis factor receptors following traumatic brain injury. J. Neurosci. 19, 6248–6256.
Sutula, T., Cascino, G., Cavazos, J., Parada, I., Ramirez, L., 1989. Mossy fiber synaptic reorganization in the epileptic human temporal lobe. Ann. Neurol. 26, 321–330.
Swanson, T.H., Sperlin, M.R., O'Connor, M.J., 1998. Strong paired pulse depression of dentate granule cells in slices from patients with temporal lobe epilepsy. J. Neural Transm. 105, 613–625.
Tauck, D.L., Nadler, J.V., 1985. Evidence of functional mossy fiber sprouting in hippocampal formation of kainic acid-treated rats. J. Neurosci. 5, 1016–1022.
Temkin, N.R., 2001. Antiepileptogenesis and seizure prevention trials with antiepileptic drugs meta-analysis of controlled trials. Epilepsia 42, 515–524.
Temkin, N.R., Dikmen, S.S., Winn, H.R., 1998. Clinical trials for seizure prevention. Adv. Neurol. 76, 179–188.
Tong, W., Igarashi, T., Ferreiro, D.M., Noble, L.J., 2002. Traumatic brain injury in the immature mouse brain: characterization of regional vulnerability. Exp. Neurol. 176, 105–116.
Tuff, L.P., Racine, R.J., Adamec, R., 1983. The effects of kindling on GABA-mediated inhibition in the dentate gyrus of the rat. I. Paired pulse depression. Brain Res. 277, 79–90.
Waldbaum, S., Dudek, F.E., 2005. Parametric assessment of the consistency of the paired-pulse protocol for studying hippocampal inhibition and hyperexcitability. Soc. Neurosci. Abstr. 31, 276.12.
Waldbaum, S., Dudek, F.E., 2007. Increased paired-pulse suppression after slight increases in excitability or reductions in GABAA-receptor mediated inhibition: does the paired-pulse technique provide artifactual evidence for "hyperinhibition" during epileptogenesis? Epilepsia 48 (S6), 118.
Winokur, R.S., Kubal, T., Liu, D., Davis, S.F., Smith, B.N., 2004. Recurrent excitation in the dentate gyrus of a murine model of temporal lobe epilepsy. Epilepsy Res. 58, 93–105.
Wuarin, J.P., Dudek, F.E., 1996. Electrographic seizures and new recurrent excitatory circuits in the dentate gyrus of hippocampal slices from kainate-treated epileptic rat. J. Neurosci. 16, 4438–4448.
Wuarin, J.P., Dudek, F.E., 2001. Excitatory synaptic input to granule cells increases with time after kainate treatment. J. Neurophysiol. 85, 1067–1077.